Climatic Change (2007) 80:301–321
DOI 10.1007/s10584-006-9120-8

Climatic impacts of historical wetland drainage in Switzerland

N. Schneider · W. Eugster

Received: 10 October 2004 / Accepted: 24 March 2006 / Published online: 4 November 2006

Abstract The effects of historical land-use and land-cover changes on the climate of the Swiss Plateau in the different seasons were investigated. In the 19th century, a civil engineering project was initiated to reshape the lake and river system on the Swiss Plateau in order to ban the frequent flooding during extreme weather events. The landscape modifications consisted primarily of a conversion of wetlands with extended peat soils into a highly productive agricultural landscape. Historical maps (1800–1850) served as a basis for the reconstruction of the past land use. The "Lokal-Modell" of the Consortium for Small-Scale Modelling was used to conduct eight one-month long high-resolution simulations ($1.5 \times 1.5\,\mathrm{km}^2$) with present and past landscape conditions. The modified soil and surface properties led to distinctly altered energy and moisture exchanges at the surface and as a consequence affected the local and regional climate. The climatic changes show different characteristics and magnitudes in the cold (October – March) as compared to the warm season (April – September). The landscape modifications led to an average daytime cooling between $-0.12\,^{\circ}\mathrm{C}$ (January) and $-0.61\,^{\circ}\mathrm{C}$ (April) and a night-time warming of $0.19\,^{\circ}\mathrm{C}$–$0.34\,^{\circ}\mathrm{C}$. The differences in the mean monthly temperatures show a warming of $0.1\,^{\circ}\mathrm{C}$–$0.2\,^{\circ}\mathrm{C}$ in the cold season and a cooling of similar magnitude in most of the study area in the warm season. The modification of the radiation budget and the surface energy balance distinctly affected the convective activity in the study area in the warm season, but had only a weak effect on convectivity in the cold season. The cloud coverage in the warm season is therefore distinctly reduced compared to the past.

Keywords Land-use change · Surface energy budget · Albedo effect · High-resolution regional climate modeling

N. Schneider
Institute of Geography, University of Bern, Switzerland
e-mail: nicolas.schneider@gmx.ch

W. Eugster (✉)
Institute of Plant Sciences, Swiss Federal Institute of Technology, ETH Zentrum LFW C55.2, CH-8092 Zurich, Switzerland
e-mail: werner.eugster@ipw.agrl.ethz.ch

1 Introduction

It is beyond doubt that the Earth's surface has been modified by humans since prehistoric times (e.g. Brown 1999; Jahns 2000; Gobet et al. 2003; Ohlendorf et al. 2003; Poska et al. 2004). At first through the use of fire to hunt game, later on through the clearance of patches of land for livestock and agriculture (e.g. Clement and Horn 2001; Fyfe et al. 2003). Over the last few centuries, the anthropogenic impact on the landscape has increased enormously both in intensity and scale, mainly through the expansion of agriculture, which has been the most significant historical change in land cover (e.g. de Sherbinin 2002).

It is now widely recognized that land-use changes on the current scale may significantly contribute to the changes of the local, regional, or even global climate (e.g. Chase et al. 2000). Even though many of the landscape changes are only local or regional, or occur only slowly over long time periods, they are, in sum, an important factor of the global environmental change (e.g. Chase et al. 1996; Govindasamy et al. 2001). On a local to regional scale, that is in the context of this paper an area of 10^4 km^2 or larger (Kustas et al. 2003; Cleugh et al. 2004), land-use changes may even have a stronger effect on the climate than larger-scale changes associated with the global greenhouse warming (Stohlgren et al. 1998; Chase et al. 2001). Pielke et al. (1999) found that the historically documented anthropogenic land-use changes in South Florida induced modifications of the local to regional weather patterns that are of comparable magnitude to the observed climatic changes during the 20th century. Baidya Roy et al. (2003) could show that since 1700, land-cover changes produced a significant cooling effect of more than 1 °C in parts of the Great Plains and Midwest as agriculture expanded and replaced grasslands.

In order to better understand regional climate modifications induced by landscape changes, it is of utmost importance to understand both the past and the future impacts of changes in land cover on the climate system. With the knowledge gained from studies investigating historical land-use changes, the impact of projected land-use and land-cover changes on the climate can more accurately be assessed.

In the evolution and development of agriculture in European countries, the drainage of wetlands has played an important role (CEC 1995). In the past, wetlands were considered wasteland, and many of the European wetlands were drained or filled in so that they could be farmed or built upon. Preferably, low-lying areas, which in former times consisted of vast stretches of marshes and bogs, and areas which were often inundated by floods were drained. However, the knowledge about the climatic impact of this kind of historical landscape changes on weather and climate is still very limited, especially on smaller scales (meso-γ) of a few hundred km^2 that are most relevant for the inhabitants of a region.

A typical example of such historical land-use and land-cover changes occurred in the late 19th and early 20th century on the Swiss Plateau after a civil engineering project was started in 1868 to drain the frequently inundated plains. In our study, we investigated the impact of these landscape modifications on the local to regional climate. For this purpose, a limited area atmospheric prediction model with a grid interval of 1.5 km^2 was used. In contrast to other studies assessing the impacts of the drainage of marshes and peatland on the climate (Venäläinen et al. 1999; Mölders 2000; Schneider et al. 2004), which were restricted to summer conditions only, our study investigates the climatic response of the land-use and land-cover changes in all seasons of the year.

2 Model, study area, and data

In our study, we used version 3.2 of the limited area atmospheric prediction model "Lokal-Modell" (LM) of the Consortium for Small-Scale Modelling (COSMO). The LM is explicitly designed for operational numerical weather prediction as well as scientific applications. It covers the meteorological meso-γ and the meso-β scales, i.e. horizontal grid intervals from 500 m to 50 km.

Four one-month long simulations for January (Jan), April (Apr), July (Jul), and October (Oct) 1998 were carried out using the physical properties of the surface and the soil given by the present land use. Analysis data from the corresponding month served as initial and boundary conditions for these simulations. Independent observational data which were not used to drive the model could therefore be used to validate the model's ability to reproduce the local to regional climate.

Additionally, four one-month long simulations with historical land-use and land-cover conditions were conducted. Here, soil and surface properties derived from the reconstructed land use in the area of direct land-use changes were prescribed to the model. The same present-day analysis data as for the simulations with present land-use conditions were used as initial and boundary conditions.

A part of the difficulty studying both the past and the future impacts of changes in land cover on the climate system is isolating the effect of local or regional land-cover changes from effects exerted by other anthropogenic and natural forcings. We therefore chose a modelling approach where the concurrent external forcings (e.g. radiative forcing of CO_2 and other trace gases, solar flux, aerosols) were kept unchanged for the different points in time that were considered. The simulations for the past conditions are therefore not supposed to reflect the observed historical climate. However, with this experiment setup we were able to isolate the changes in the atmosphere due to the historical land-use changes in the study area from all other extrinsic effects.

2.1 Model setup

Details on LM can be found in Schneider and Eugster (2005). The only difference is that here we applied LM in different seasons.

The model domain extends over approximately $160 \times 200\,\mathrm{km}^2$ and covers Western Switzerland and parts of France (Figure 1). The horizontal grid interval is $1.5\,\mathrm{km} \times 1.5\,\mathrm{km}$. In the vertical, 45 layers are used, reaching a height of more than 23 km. The lowest 2 km of the atmosphere are represented with at least 18 layers in order to adequately resolve vertical structures in the boundary layer. All simulations were run with a time step of 10s and output was written every hour. In order to allow the model to spin up, the first day of each simulation was not used for validation and analysis purposes.

3-hourly ECMWF operational 4DVAR analysis data of all months considered were used as initial and boundary conditions for LM runs with a 7 km mesh size. From these simulations, the initial state and 1-hourly boundary fields of the atmosphere and the soil were obtained for the high-resolution simulations. Identical initial and boundary conditions were used for the simulations with the past or the present land use apart from soil moisture, which was modified to allow for the different soil types in order to achieve realistic soil conditions. Thus, soil moisture in the area of land-use changes was generally higher for the past simulations compared to the corresponding simulations with present land use due to a much higher fraction of porous peat soils during past conditions.

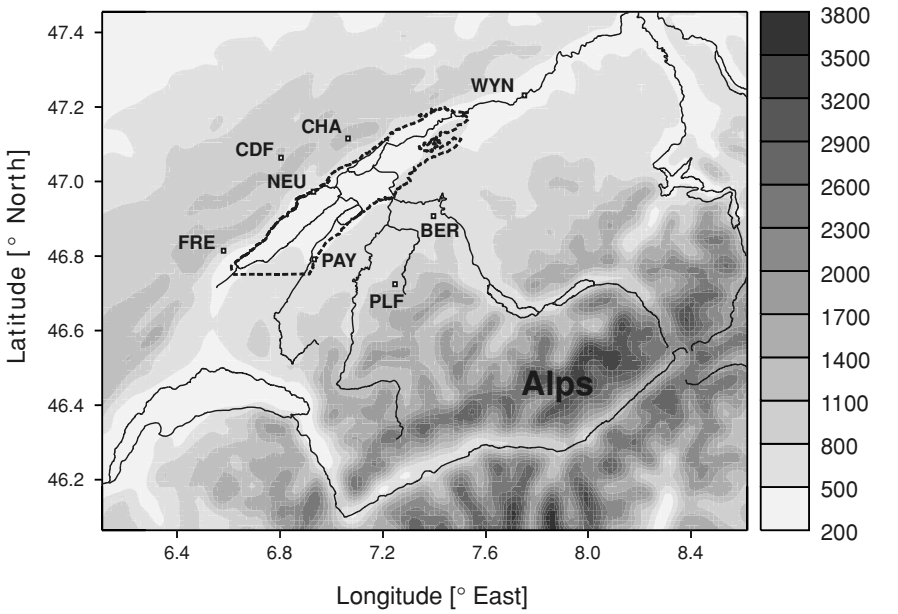

Fig. 1 Topography of the model domain (scale at right in m a.s.l.). The extent of the model domain is approximately $160 \times 200\,\mathrm{km}^2$. It comprises most of the Swiss Plateau, parts of the Jura mountains in the Northwest, and parts of the Alps in the Southeast. The broken line denotes the extent of the study area where the landscape was modified by the wetland drainage. The thin lines give major lakes and rivers within the domain. Meteorological stations referred to in the text are: Bern (BER), Chasseral (CHA), La Chaux-de-Fonds (CHF), La Frétaz (FRE), Neuchâtel (NEU), Payerne (PAY), Plaffeien (PLF), and Wynau (WYN)

2.2 Study area, land-use and soil data

The actual study area is defined as the area where the landscape was modified due to the drainage of the wetlands. It is located on the Swiss Plateau in the northwestern part of the model domain (Figure 1) and comprises three major lakes. Until the middle of the 19th century, the plains around the three lakes were frequently inundated and marsh lands were dominant. In the central area between the three lakes, a blanket peat bog area of approximately 400 km^2 existed. In 1868, the leveeing and draining of the formerly marshy and frequently inundated plains had started. The adjustment of the lake and river system lowered the mean levels of the three lakes by 2.5 m. Subsequently, the large bog area between the three lakes was converted into intensively used agricultural land. At present, the region is one of the most important and productive agricultural areas in Switzerland. Schneider et al. (2004) give a more detailed description of the current land use and soils in the study area.

The present land-use types in the model domain are obtained from Swiss National Land Census data collected between 1992 and 1997 and the USGS Global Land Cover Characteristics Data Base Version 2.0 with the IGBP Land Cover Legend (Loveland et al. 2000). After the aggregation of both data sets to a grid interval of 1.5 km × 1.5 km, the present conditions are represented by a total of 21 land-use classes.

The historical land use in the area with direct modifications due to the drainage of the wetlands was reconstructed from historical maps originating from the period 1800–1850. During the reconstruction process, 8 land-use classes could be distinguished, of which 7 remained after the data set was aggregated to the coarser grid interval. Four out of these 7

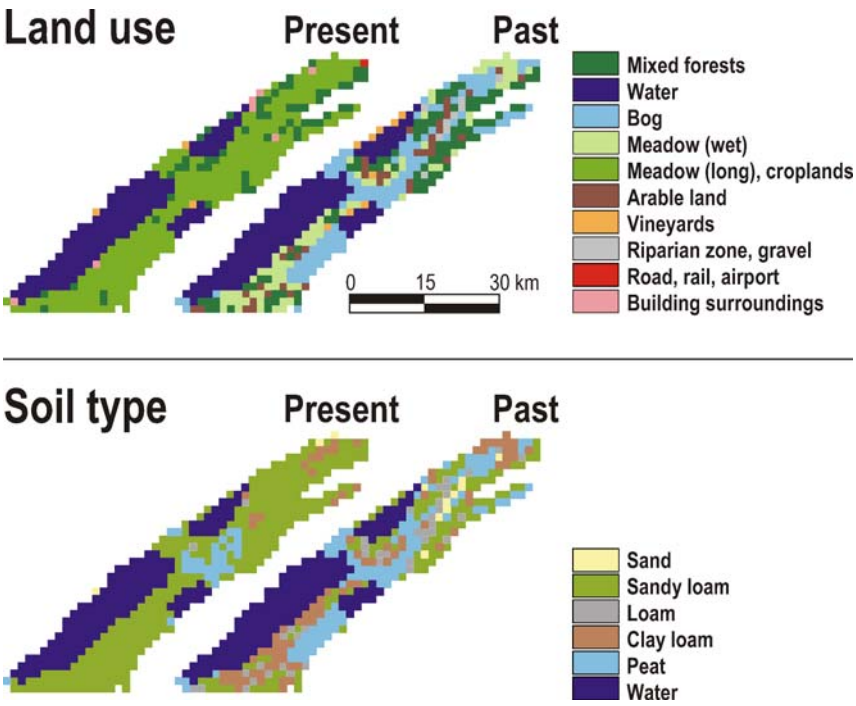

Fig. 2 Present and past land use (top) and soil types (bottom) in the study area at model grid interval

classes directly corresponded to one of the present land-use classes. Hence, only three additional land-use classes had to be introduced to represent the historical land use, resulting in a total of 24 land-use classes that were used to account for the present and past landscape characteristics in the model domain. Figure 2 (top) shows the present and the past land-use types. The changes in the land use show a transition from a rather heterogeneous past landscape which was dominated by bog and wet meadows to a rather homogeneous present landscape with predominantly agriculturally used meadows and croplands. The most important land-use changes are from bog to meadows or crops (34%), from wet meadows to agriculturally used meadows and crops (22%), and deforestation (14%). Finally, the parameters describing the vegetation (albedo, leaf area index, fractional plant coverage, plant rooting depth) and the surface roughness were assigned to the specific land-use type (see Appendix A and Table A.1).

Figure 2 (bottom) shows the present and the past soil types in the study area. The present soil types used in the LM were derived from Swiss National Land Census data on the suitability of the soils for agricultural use (Frei et al. 1980). Here, the soil texture information was best suited to determine the present soil type. For past conditions, the soil type had to be derived from the dominant land-use type due to the lack of high-quality soil information for the 19th century. This approach assumes that soil properties and vegetation and hence the type of land use are strongly correlated. This approach is supported by the fact that before the drainage of the wetlands, the soils and the vegetation in the study area evolved over several hundred years without being significantly affected by intensive agricultural use. Thus, an equilibrium between soil properties and land-use type describing the vegetation may be a realistic assumption.

The modifications of the landscape therefore also lead to distinctly altered soil properties, indicated by a lower present soil heat capacity $c_p(\Delta c_p = -0.26 \cdot 10^6\,\mathrm{J\,K^{-1}\,m^{-3}})$ and a higher soil thermal conductivity $\lambda(\Delta\lambda = +0.39\,\mathrm{WK^{-1}\,m^{-1}})$. The present-day average pore volume (fraction of volume) is lower by 0.1.

3 Results

3.1 Model validation

The model performance with the current high-resolution setup was validated with independent station data from the Swiss Meteorological Network (ANETZ). The four simulations with the present land use and the present soil conditions were compared with measurements from the corresponding months. The model validation thereby focussed on the atmospheric conditions in the area that amply comprises the study area. Thus, the measurements of eight stations within an extended perimeter around the study area were averaged in order to get representative values for the atmospheric conditions in this area (for the station locations see Figure 1). In the same manner, the simulated values at the grid cells corresponding to the station locations were averaged.

Figure 3 shows the comparison of the averaged observed and simulated air temperature (left) and mixing ratio (right) for all simulations with present soil and surface conditions in 1998. In all months, the temperature changes over several days due to the changing synoptic weather conditions as well as extreme values and therefore also the daily amplitudes are well captured. The correlations between observed and simulated temperatures are excellent with a correlation cofficient ranging between 0.91 (October) and 0.96 (July).

The mixing ratio is simulated with a somewhat lower skill than temperature. Too large a daily amplitude of the mixing ratio is simulated on a few days, mainly in July. Nevertheless, the model reproduces most of the diurnal variations as well as the day-to-day changes very realistically. Here, the correlation coefficients between the observations and the simulations are 0.95, 0.82, 0.96, and 0.91 for January, April, July, and October (hereafter abbreviated as JAJO), respectively. In all months, the root mean squared error (RMSE) is below 1 g $\mathrm{kg^{-1}}$.

In Figure 4, the comparison of the simulated values with the observations are shown for precipitation and wind speed. The simulated precipitation generally agrees well with the observed amounts. Although no convection parameterization was applied, the model is able to correctly predict both the temporal occurence and the intensity of the precipitation. This indicates that most of the convection is explicitly resolved on the very small grid scale used in this study. Only in April, the precipitation is slightly underestimated.

A good correspondence with observed values is also found for the simulated wind speed. Both the diurnal variations as well as the variations throughout the months are nicely captured. The correlation coefficients between observations and simulated values range from 0.81 (April) to 0.96 (October). Moreover, the simulated and measured values of the wind direction also agreed well (not shown). For the wind direction, the correlation coefficients are 0.91, 0.62, 0.74, and 0.79 for JAJO, respectively. The RMSE for the wind direction is between 30° (January) and 43° (July). Altogether, the validation of the model results shows an adequate model performance for the purpose of this study.

3.2 Changes in the radiation budget and the surface energy balance

The changes in the vegetation and soil properties due to the land-use and land-cover changes in the study area distinctly affected the radiation budget and the surface energy

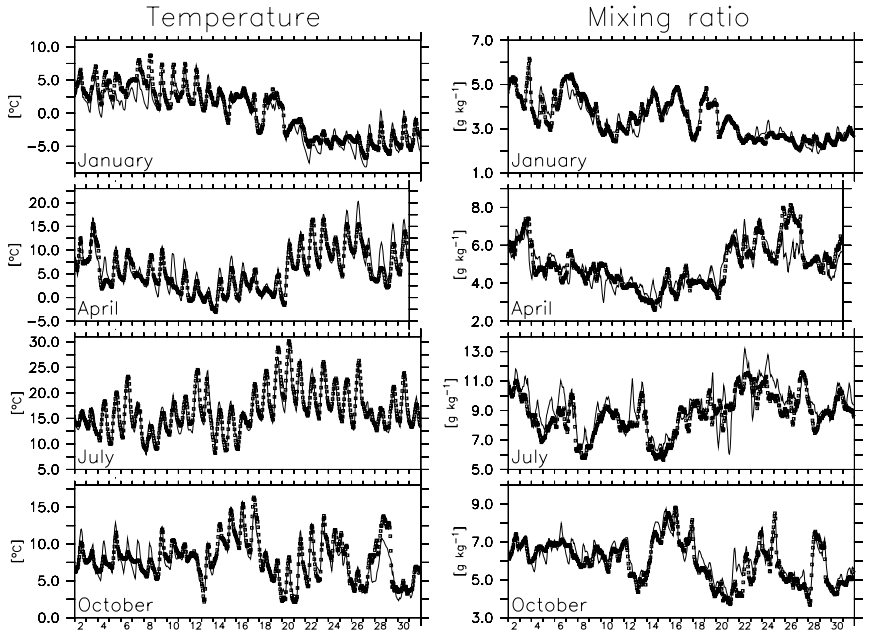

Fig. 3 Comparison of measured (open squares) and simulated (solid line) temperature [°C], and mixing ratio [g kg^{-1}] for JAJO 1998, respectively. Shown are the averaged measurements from eight sites of the Swiss Meteorological Network within or close to the study area and the averaged simulated values of the grid cells corresponding to the station locations (cf. Figure 1). Time interval for both measurements and simulated values is one hour

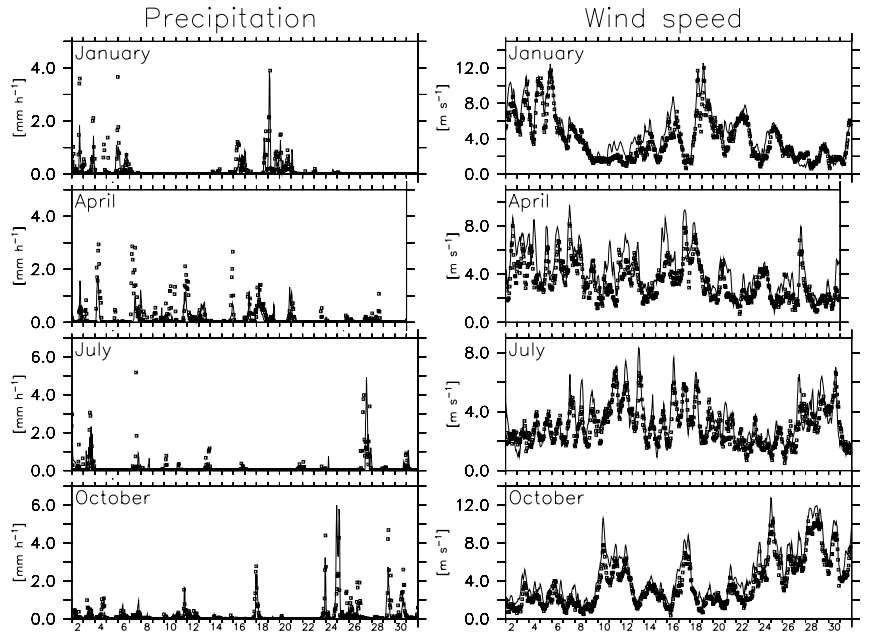

Fig. 4 Same as Figure 3 but for precipitation and wind speed

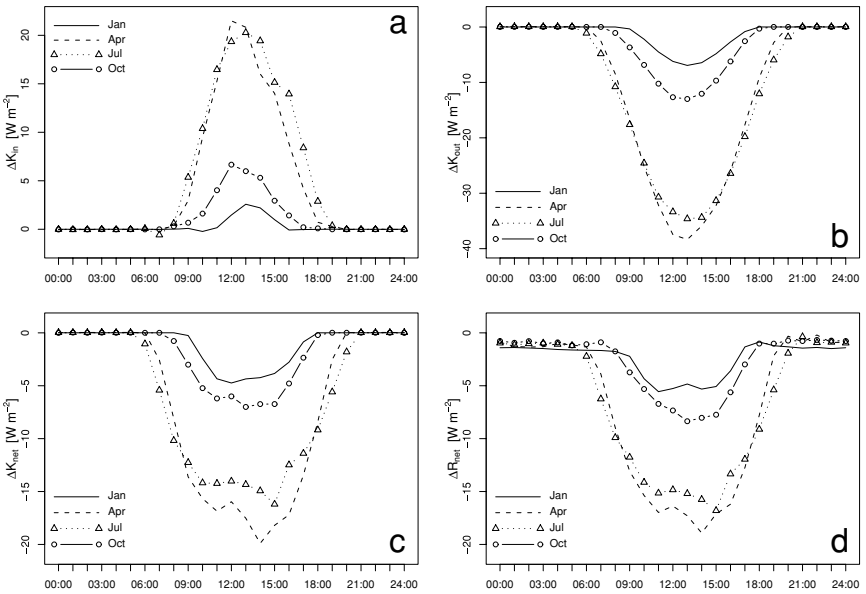

Fig. 5 Differences (present–past) in the mean diurnal cycles of (a) the incoming and (b) reflected shortwave radiation, (c) the net shortwave radiation and (d) the net radiation averaged over the area of land-use changes for all simulated months in 1998. K_{in}: incoming shortwave radiation; K_{out}: reflected shortwave radiation; K_{et}: Net shortwave radiation; R_{net}: Net radiation. Radiation fluxes to the surface are positive while radiation fluxes from the surface are negative

balance. Through the altered exchange of water and energy, these changes in the radiation budget and the surface energy balance also induced changes in the regional climate.

Figure 5 shows the changes in the mean diurnal cycles of the radiation budget components for every simulated month as a spatial average over the study area (Figure 1). A daytime increase (present – past) in the incoming shortwave radiation is simulated in all months (Figure 5a). In April and July, a similar maximum daytime increase of approximately 20 Wm^{-2} is simulated, whereas in January and October, the maximum differences only amount to 3 and 7 Wm^{-2}, respectively. These increases can only result from a reduced cloud cover since the top-boundary incoming shortwave radiation is identical for the present and the past simulation of a specific month. Futhermore, the effects of other absorbers (CO_2, O_3, aerosol) were kept constant.

Like for the incoming shortwave radiation, April and July show similar differences for the reflected shortwave radiation. The maximum increases in the reflected shortwave radiation (Figure 5b) are 38 and 35 Wm^{-2} in April and July, respectively, whereas the maximum increases in January and October are 7 and 13 Wm^{-2}, respectively. The changes in the reflected shortwave radiation are a result of the albedo effect and can be fully explained by the nowadays higher total albedo in all months.

The resulting differences in the net shortwave radiation (-6, -19, -17, -8 Wm^{-2} in JAJO, respectively) are very similar to the changes in the net radiation (Figure 5, c and d). Thus, the solar terms are the dominant components, at least during daytime since changes in the net longwave radiation only contributed a little to the changes in net radiation (not shown). In general, differences in the radiation budget components are similar in April and

July, i.e. during the growing season, which in this region roughly spans the months from April to September. Hereafter, we also refer to this period as *warm season*. During the time of low vegetation activity (October to March, hereafter *also cold season*), the differences in the radiation budget components are distinctly smaller.

Figure 6 shows the changes in the mean diurnal cycles of the sensible and latent heat fluxes as well as the ground heat flux for all simulated months. Due to the nowadays lower net radiation during the day (Figure 5d), the present-day sensible heat fluxes are lower in all simulated months. The maximum decreases in QH are −5, −39, −24, and −8 W m^{-2} in JAJO, respectively. The present-day latent heat fluxes are lower in all months apart from April. During the growing season, the plant transpiration distinctly contributes to the total evapotranspiration. In April, the average fractional plant coverage is nowadays clearly higher (+0.14; +26%) and therefore leads to an enhanced daytime plant transpiration at present compared to the past. Therefore, the difference in QE (present – past) is negative in the beginning of the day when plant transpiration is still low and the higher fractional plant coverage does not have a strong effect yet compared to the reduction of the net radiation. In the afternoon, however, when plant transpiration is high, the difference in QE rapidly becomes positive. In contrast to April, the fractional plant coverage in July is slightly lower (−0.02). Although the present-day fractional plant coverage is also distinctly higher in January and October, the vegetation shows very little activity during this time of the year and therefore only contributes a little to the total evapotranspiration.

Furthermore, no water stress conditions were modelled for the vegetation due to the still high water availability in the present soils. In this case, the evaporation does not primarily depend on soil moisture controls on vegetative conductance. Smith et al. (1992) could show that above a soil moisture threshold of 25% by mass, the evaporative fraction defined as the ratio between evaporation (QE) and available energy (= net radiation – QG) was nearly constant. In our study area, the soil moisture is close to or above that threshold for most of the simulated days also for present conditions. Furthermore, Stewart and Verma (1992) found that the evaporative fraction is also insensitive to the leaf area index above that threshold. Therefore, the changes in the leaf area index, which are most pronounced during July, do not exert a dominant impact on QE.

If the sum of QE and QH, i.e. the turbulent heat fluxes into the atmosphere, is considered, a reduction is simulated for all months. Reductions of −14 and −19 W m^{-2} occur in January and October, respectively, whereas distinctly larger reductions are simulated in April and July (−34 and −33 W m^{-2}).

Apart from the reduction in net radiation, an important reason for the lower present-day turbulent heat fluxes into the atmosphere is the modification of the soil properties. During the night, the present-day upward ground heat flux is higher by 3 to 5 W m^{-2} compared to the past. During the day, the downward ground heat flux is nowadays enhanced by up to 17 and 18 W m^{-2} in April and July, and by up to 9 and 12 W m^{-2} in January and October. This can be explained by a higher present-day soil thermal conductivity λ combined with a lower soil heat capacity c_p of the present soils. In contrast to the high organic peat soils that dominated in the past, the present-day soils are physically more similiar to mineral soils. The present-day daytime heat transfer to the lower soil layers is therefore higher, and less heat is concentrated in the uppermost soil layer during the day. This results in distinctly lower soil temperatures at the surface (Figure 7c). In contrast to the daytime conditions, the nowadays persistantly higher upward ground heat flux during the night (Figure 6c) leads to present soil temperatures at the surface that are between 0.2 and 0.4 °C higher than in the past.

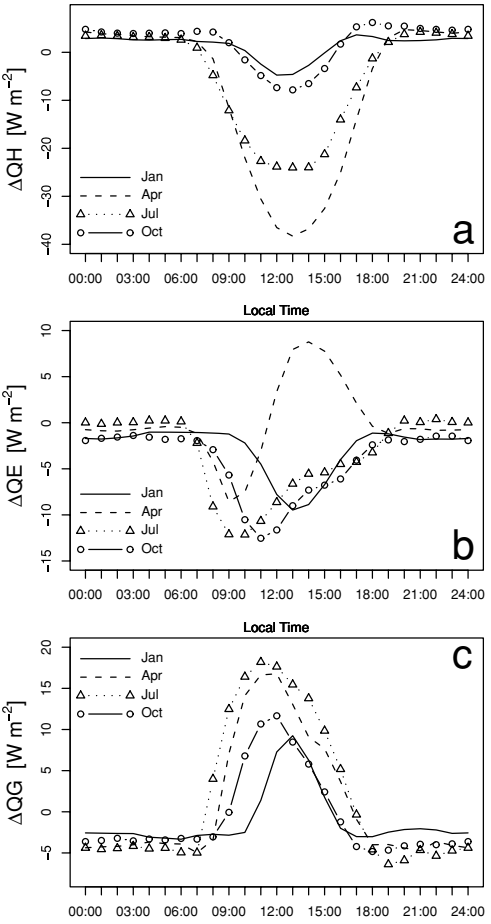

Fig. 6 Same as Figure 5 but for (a) sensible, (b) latent, and (c) ground heat flux. QH: sensible heat flux, QE: latent heat flux, QG: ground heat flux. Heat fluxes from the surface are positive while heat fluxes to the surface are negative

3.3 Changes in temperature and humidity

As a result of the changes in the radiation budget and the surface energy balance, the air temperature and the humidity of the air were also altered.

Figure 7a shows the difference (present – past) in the air temperature at screen height (2 m) averaged over the study area. A daytime cooling and a night-time warming resulted in all simulated months. The most pronounced daytime cooling was modelled for April with a maximum cooling of −0.61 °C, followed by July (−0.28 °C), January (−0.22 °C), and October (−0.12 °C). During the night, the simulated temperature differences due to the landscape modifications show less variance. The maximum increases in the temperature averaged over the study area are in the range from 0.19 (Oct) to 0.34 °C (Jul). In summary, the diurnal temperatue range (DTR) averaged over the study area changed by −0.57, −0.96, −0.62, and −0.40 °C in JAJO, respectively.

The monthly mean air temperature averaged over the entire study area changed by 0.18, −0.07, 0.05, and 0.10 °C in JAJO, respectively. In areas with deforestation, the mean monthly temperature increased by at least 0.5 °C in all simulated months. The temperature changes in those parts of the study area where bog was replaced by meadows or croplands

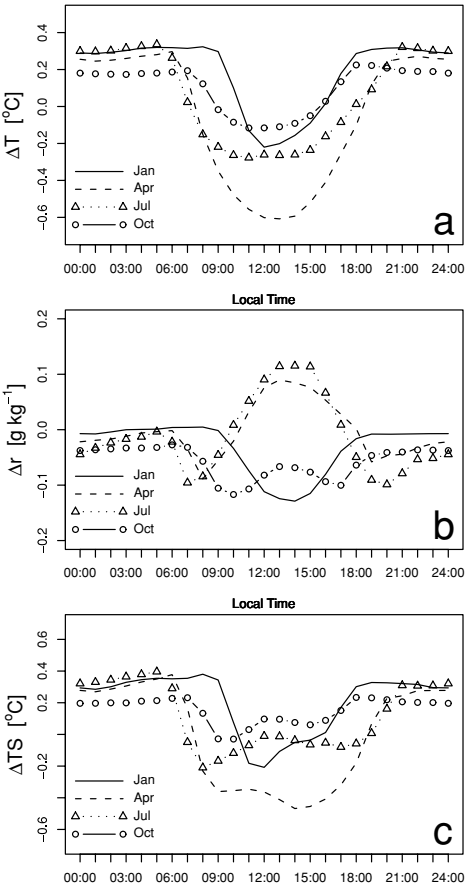

Fig. 7 Same as Figure 5 but for (a) air temperature, (b) mixing ratio, and (c) surface temperature. T: air temperature at 2 m; *r*: mixing ratio at 2 m; TS: surface temperature

were 0.28, −0.15, −0.06, and 0.14 °C in JAJO, respectively. In general, warmer conditions were simulated in the entire study area during the cold season, whereas during the warm season a cooling was simulated all over the study area apart from the deforested part. Although with snow cover present, the albedo in deforested areas is higher than in forested areas, this only had a minor effect on the temperature since there is normally no permanent snow cover in the study area. In this part of Switzerland, mild oceanic winters are predominant.

The warmer night-time conditions also influenced the freeze conditions in the study area. Under past land-use conditions, the duration of periods of sub-zero temperatures ($T < 0\,^{\circ}C$) averaged over the study area was 277.9 hours in January and 8.4 hours in April. In contrast to past conditions, sub-zero temperatures in the study area under present land-use conditions only occurred during 266.6 and 5.0 hours on average in January and April, respectively. This corresponds to relative changes of −4.1% (Jan) and −40.5% (Apr). Due to the limited length of periods with freezing conditions in April, the large relative change just expresses that this type of land-use changes shifted April more towards frostless months. Conversely, in January, the change in the duration of periods of sub-zero temperatures gives a good measure for the impact of the land-use and land-cover changes on the freezing conditions in the study area.

Temperature changes were also simulated several hundred meters above ground in the study area. Figure 8 shows the mean nocturnal and daytime changes (present – past) in the

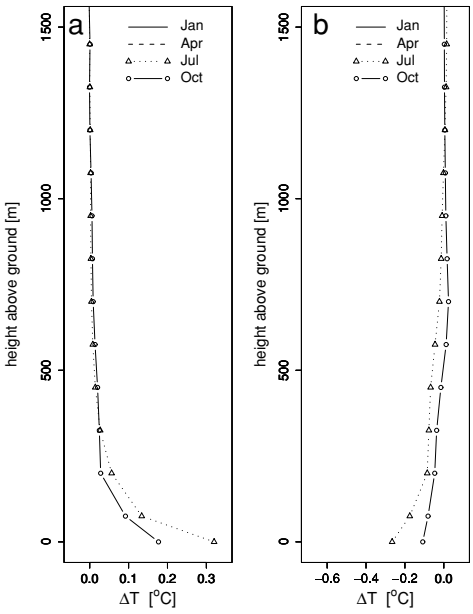

Fig. 8 Differences (present – past) in the mean daytime and nocturnal vertical profiles above the area of land-use changes of the air temperature (T) for all simulated months in 1998. (a) nocturnal changes (average from 3–6 CET); (b) daytime changes (average from 11–14 CET)

vertical profile of the air temperature above the study area. During the night, the positive temperature differences are constrained to a rather shallow layer of 200–300 m thickness, i.e. the stable nocturnal surface layer where CO_2 accumulates (Eugster and Siegrist 2000). In January, temperature differences are only simulated in the lowest 100 m above ground. During the day, noticeable negative temperature differences in the convective mixed layer exist up to a height of approximately 500–700 m above ground in the warm season and up to a height of approximately 200–300 m above ground in the cold season.

The differences in the humidity at screen height (Figure 7b) are most pronounced during the day, when changes in the net radiation led to noticeable changes in the latent heat flux. The changes in the diurnal cycle of the near-surface humidity show similar characteristics for April and July, i.e. the months within the growing season when the present-day higher transpiration by agricultural plants is relevant, and for January and October when the vegetation is inactive.

Relevant differences in the vertical profile of mixing ratio of the air (not shown) were only found during the daytime phase, and were most pronounced during the growing season. In January and October, weak negative differences were simulated throughout the lowest 300–500 m above ground during the day. In April and July, however, the mixing ratio in the lowest 200 m above ground is nowadays higher than in the past, but lower above that. The maximum decrease in moisture in these months was simulated at a height of about 600–700 m above ground.

3.4 Changes in convection, cloud coverage, and precipitation

The interaction mechanisms between the surface and the atmosphere play a crucial role regarding the development of convective cells, the cloud coverage, and consequently of cumulus convective rainfall. Any aspects of landscape characteristics which influence the heating and moistening of the atmospheric boundary layer will therefore affect the potential for cumulus convective rainfall (Pielke 2001). Thus, the changes in the radiation budget and

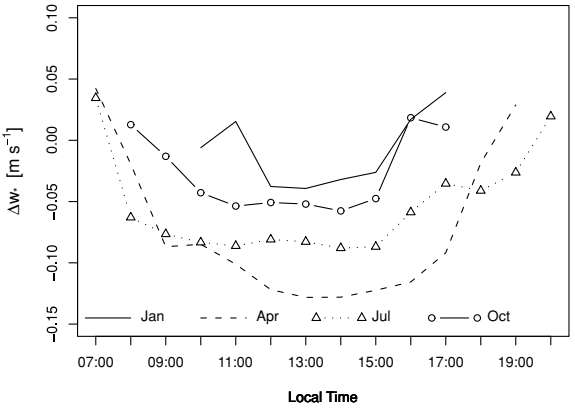

Fig. 9 Differences (present – past) in the mean daytime convective velocity scale, w_*, averaged over the study area

the surface energy balance components may alter the cloud-radiation-precipitation feedback mechanisms in the study area.

In order to better understand the impacts of the landscape modifications on convection, the cloud coverage, and hence precipitation, the mixed layer height, z_i, and the convective velocity scale, w_*, were diagnostically calculated for all simulated months. w_* is a velocity scale describing the strength of vertical convection in the mixed layer (see Appendix B). Figure 9 shows the daytime differences (present – past) in the convective velocity scale averaged over the study area. During the day, w_* is nowadays lower than in the past for all simulated months. In the cold season, changes in w_* are only small and limited to a few hours around noon, whereas in the warm season, distinctly larger changes in w_* were simulated. In the latter two months, the maximum negative differences in w_* correspond to relative changes of approximately -10%. Therefore, a reduced buoyancy and hence less active convective thermals were simulated for the present conditions during April and July. This is in agreement with the simulated decrease in QH and the lower near surface air temperature, which also indicate a weaker formation of convective thermals. In contrast to the warm season, the changes in w_* in January and October are comparably small.

The simulated changes in the mixed layer height for the cold and warm season (Figure 10, a and b) are in accordance with the changes in w_* and hence the convective activity. In the cold season, the average daytime z_i over the study area is slightly lower (Figure l0a), the largest differences being approximately 30 m. In the warm season, however, distinctly larger decreases in z_i are simulated over a larger part of the study area as compared with the cold season, the largest differences in the average z_i being roughly 90 m.

Figure 10 (c and d) shows the mean daytime differences in the cloud coverage for the cold and the warm season. In the cold season, only small differences in the average cloud coverage of up to 2.5% were modelled. Furthermore, these differences are limited to the extent of the study area. In contrast to that, the reduction in the cloud coverage is much more distinct during the warm season, when the average daytime cloud coverage is nowadays up to 5% lower than in the past. During this period, the reduction of the cloud coverage was also simulated in the downwind areas in the west of the study area, with diminishing differences in the cloud coverage with increasing distance from the study area.

Finally, Figure 10 (e and f) presents the relative differences in the total monthly precipitation for the cold and the warm season. Here, it can be seen that the landscape modifications led to a decrease in precipitation of up to 5% during the cold season. Then, the decrease in

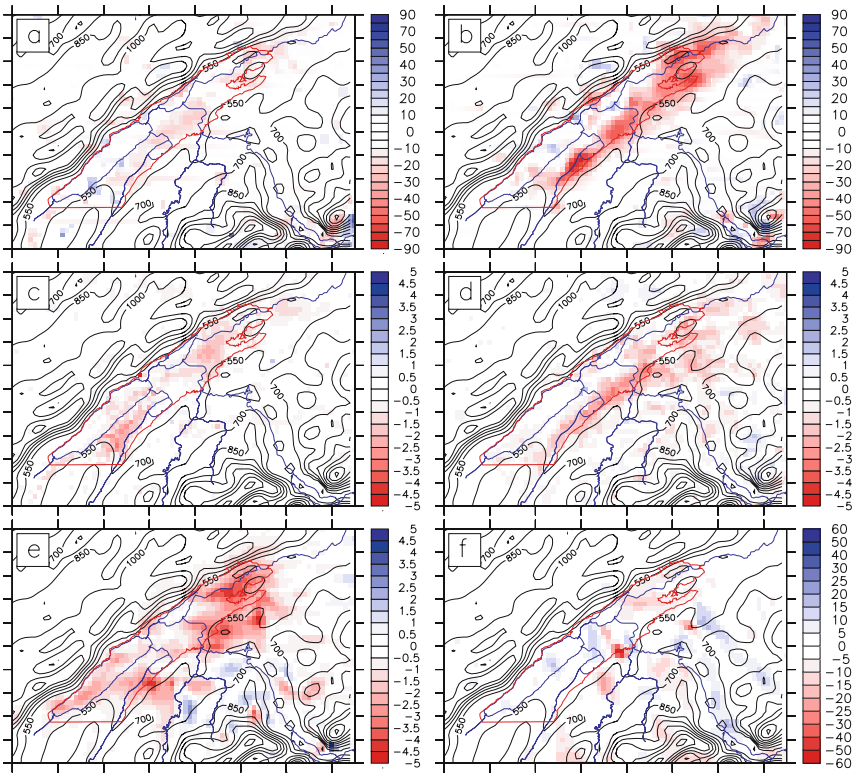

Fig. 10 Absolute differences (present – past) in the daytime mixed layer height (a, b) and the daytime cloud coverage (c, d) as well as relative differences in the total monthly precipitation (e, f) for the cold season (average of Jan. and Oct., left column) and the warm season (average of Apr. and Jul., right column). (a) mean daytime (average from 11–14 CET) difference in the mixed layer height [m] averaged over Jan. and Oct.; (b) same as a, but for Apr. and Jul.; (c) mean daytime (average from 11–14 CET) difference in the total fractional cloud coverage [%] averaged over Jan. and Oct.; (d) same as c, but for Apr. and Jul.; (e) relative difference in the total monthly precipitation [%] averaged over Jan. and Oct.; (f) same as e, but for Apr. and Jul.

precipitation is rather homogeneous over the study area itself and downwind areas adjacent to the study area. In contrast to that, the changes in precipitation in the warm season are much wider spread in space and show large local extremes. Local hot spots of changes of up to 60% were simulated, indicating that in April and July, the landscape changes distinctly affected the local convective cycles. However, the amount of precipiation for the whole domain remained virtually unchanged.

4 Discussion

The replacement of the wetland vegetation and forests by croplands and meadows increased the albedo in all simulated months. The higher albedo led to a decrease in the vertical turbulent fluxes of sensible and latent heat (see also Mölders 2000) as a consequence of the reduced present-day net shortwave radiation at the surface. The simulated reduction of the sensible

heat fluxes during the day caused a relative daytime cooling in the mixed layer, which is most pronounced in April and weaker during the cold season (Figures 7 and 8).

The daytime cooling in the study area, however, was not only caused by the initial change in albedo. Through the distinct increase in the fractional plant coverage in April, the present-day daytime QE is higher than in the past. The energy partitioning between QH and QE, and thus the Bowen ratio (= QH / QE), changed in favor of latent heat. This altered energy partitioning in April amplified the relative cooling effect exerted by the decrease in the net radiation via the albedo changes.

The surface air temperature is furthermore influenced by the altered soil properties, which resulted in present-day ground heat fluxes that are higher than in the past (Figure 5). This is in accordance with the study by Mölders (1999) who showed that over grassland, the temperature is lower than over marshland due to the lower heat capacity as well as the higher thermal conductivity of the grassland soils and the higher albedo of the grassland. During the night, albedo differences become irrelevant and the altered vegetation can be excluded as a cause for the temperature changes. Therefore, the present-day warmer night-time temperatures in the study area in all months are a result of the enhanced upward heat flux in the soil.

The simulated decrease in the net shortwave radiation and the resulting differences in the sensible and latent heat fluxes as well as the ground heat flux, however, did not only affect the air temperature. Cumulus cloud base height is directly related to surface heat and moisture fluxes (e.g. Rabin et al. 1990; Schrieber et al. 1996). The size of thermals generated from surface heating is a function of z_i, QH, and height within the boundary layer (McNider and Kopp 1990). Therefore, the rate of growth of the boundary layer during the day, and the entrainment of free atmospheric air into the boundary layer are both dependent on QH. The magnitude of QH is of considerable importance for various daytime atmospheric boundary-layer processes (Segal et al. 1989). Pielke et al. (1998) and Pielke (2001) showed that the depth of the planetary boundary layer becomes shallower if the sensible heat flux is reduced, a finding that is also supported by this study.

In the warm season, the reductions in QH and the turbulent heat fluxes were large enough to generate distinctly weaker buoyancy at the land surface, which finally led to the build-up of a noticeably shallower daytime mixed layer (Figure 10b). In contrast to the warm season, the vertical turbulent fluxes in the cold season and hence the daytime mixed layer height were less affected by the modified exchanges of energy and moisture since the simulated differences in QH and the turbulent heat fluxes are noticeably smaller than in the warm season. Hence, the impact of the landscape modifications on the already lower convective activity in these months is much weaker than in the warm season, leading to a distinctly smaller decrease in the daytime mixed layer height (Figure 10a). This is in agreement with the simulated daytime differences in the convective velocity scale (Figure 9), which are notably smaller in January and October compared to April and July.

The reduced upward vertical turbulent fluxes in the warm season also affect the vertical distribution of moisture. The surface moisture flux decreased, i.e. the present daytime QE is lower than in the past (Figure 6b). Thus, the surface moisture flux did not change in a manner that would explain the present-day increased near-surface humidity. The increased humidity at screen height is a consequence of the reduced upward tranpsort of moisture, which is in accordance with the maximum deficit in moisture at a height of about 600–700 m above ground.

As a consequence of the lower present-day moisture content at heights of 200–800 m above ground, the cloud coverage is also reduced (Figure 10, c and d). In the warm season, the difference in the cloud coverage is larger than in the cold season due to the stronger

decrease in humidity at heights between 500 and 700 m above ground. In this height, the present-day drier air masses are further advected downwind, which explains the decline in the cloud coverage downstream of the study area.

The reduction in cloud coverage in turn reduces the reflection of shortwave radiation by clouds and thus negatively feeds back upon the solar radiation. Consequently, the incoming shortwave radiation in the present-day simulations is higher in all simulated months (Figure 5). The stronger increase of the incoming shortwave radiation during the warm season can on the one hand be explained by the more vigorous insolation at this time of the year. On the other hand, it can be explained by the stronger decrease in the cloud coverage, i.e. the stronger decrease of atmospheric water, which reflects shortwave visible light. Due to higher present-day incoming shortwave radiation, the decline in the net shortwave radiation and thus in net radiation which are caused by the increase in albedo is approximately reduced by half (Figure 5). However, the net effect is only approximately one fourth in the cold season compared to the warm season.

Finally, the changes in convective activity, atmospheric moisture content and hence cloud coverage due to the landscape modifications affected the precipitation in the study area (Figure 10, e and f). In the cold season, precipitation changes were moderate. The landscape modifications did not exhibit a strong impact on the convective activity and therefore only affected the lowest few hundred meters of the atmosphere. Hence, only air masses that more or less remained over the study area were affected, resulting in a reduction of precipitation over the study area and adjacent areas. In the warm season, the relative precipitation changes can locally reach values that are roughly one order of magnitude larger than in January and October. A conclusive spatial pattern describing the precipitation changes is difficult to identify in these two simulated months representing the warm season. This aspect was investigated separately in a recent study (Schneider and Eugster 2005) for the summer climate only.

5 Conclusions

We showed that the changes in the soil and surface properties due to the historical land-use and land-cover changes distinctly affected the local to regional climate on the Swiss Plateau. The climatic changes show different characteristics and magnitudes in either the cold (October – March) or the warm season (April – September).

In all seasons, the present-day net radiation averaged over the study is lower than in the past, with a stronger decrease in the warm season. This decrease is due to the higher present-day albedo. The albedo effect on the net radiation is weakened by the negative feedback of the reduced present-day cloud coverage on the incoming shortwave radiation.

Larger ground heat fluxes were simulated for present conditions leading to warmer soil temperatures at the surface and also warmer near-surface air temperatures at present. These changes vary less throughout the year since the changes in the soil properties are identical for all months. Due to the warmer night-time temperatures, the duration of sub-zero temperatures in January is now reduced by 4.1%.

As a consequence of the lower present-day net radiation and the enhanced ground heat flux, less energy is available at the surface for vertical transfer in the form of turbulent heat fluxes during the day. The reduced sensible heat flux led to an average daytime cooling which is notably larger in the warm season than in the cold season. Furthermore, a pronounced decrease in the diurnal temperature range was simulated in all months. Furthermore, the reduction of the turbulent heat fluxes distinctly affected the convective activity in the study

area in the warm season, but had only a weak effect on convectivity in the cold season. Thus, the reduction in the cloud coverage due to the landscape modifications is much more pronounced in the warm season, leading to reduction in the daytime cloud coverage of up to 5%.

The landscape modifications also affected the local to regional precipitation. However, precipitation changes in the cold season only occurred in the study area or adjacent downwind regions.

Acknowledgements The authors would like to thank the Consortium for Small-Scale Modelling (COSMO) for the use of the "Lokal-Modell". We thank MeteoSwiss and the German Weather Service for their support. ECMWF operational analysis data used in this study have been obtained from the ECMWF data server. Further thank goes to the IT Department of the University of Bern for permanently providing us with 6 nodes of the 32 nodes Linux parallel computing cluster. N.S. was funded by the Swiss National Science Foundation grant 21-66927.01. This work was carried out as part of the IGBP/IHDP project on Land Use and Land Cover Change (LUCC). W.E. was also supported by a Hans-Sigrist fellowship grant from the University of Bern during the early stage of this project.

Appendix A: Vegetation parameters

The parameters describing the vegetation (albedo, leaf area index, fractional plant coverage, plant rooting depth) and the surface roughness were assigned to the specific land-use type via the use of a lookup-table (Table A.1). For the vegetation albedo α_v, four values for each of the simulated months were defined for every land-use type (Table A.1). The seasonal variation of the leaf area index *LAI* and the fractional plant coverage f_c was parameterized with a generic function X (Figure 11). This parameterization is implemented in the pre-processing program of the LM (Schättler and Doms 1999) and successfully used in the operational applications of the LM. X depends on the latitude φ, the day of the year D, and the geopotential $\Phi = g \cdot h$:

$$X(\varphi, D, \Phi) = X_{\min} + f_v(\varphi, D) \cdot f_h(\Phi) \cdot (X_{\max} - X_{\min}), \tag{1}$$

where g is the acceleration due to gravity, h is the height above sea level, and $X_{\min}$ and $X_{\max}$ are constant values at the time of low activity (Winter) and at full growth (Summer), respectively. $X_{\min}$ and $X_{\max}$ are listed in Table A.1 for f_c and LAI. f_h and f_v are a height reduction factor and a vegetation factor depending on the geographic latitude and the time of year, respectively. f_h and f_v take the following form:

$$f_h(\Phi) = e^{-5\cdot 10^{-9}\cdot \Phi^2}, \tag{2}$$

$$f_v(\varphi, D) = \max\left(0, \min\left\{1, c \cdot \sin\left[\pi \cdot \max\left(0, \frac{D - D_v(\varphi)}{D_\tau(\varphi)}\right)\right]\right\}\right) \tag{3}$$

where D_v is the starting day of the growing season, D_τ is the length of the active growing season in days, and c is a coefficient set to a fixed value of 1.12. With the above settings for f_h, the value of f_h is reduced by half at an altitude of 1200 m a.s.l. D_v and D_τ are determined as follows:

$$D_v(\varphi) = \max\{1, 3 \cdot (|\varphi| - 20^\circ)\} \tag{4}$$

$$D_\tau(\varphi) = \min\{365, 345 - 4.5 \cdot (|\varphi| - 20^\circ)\}. \tag{5}$$

Table A1 Parameters used by the LM to describe the surface roughness and the vegetation. z_0: surface roughness length; f_c: fractional plant coverage (minimum and maximum value); α_v: vegetation albedo (values for January, April, July, October); *LAI*: leaf area index (minimum and maximum value); r_d: plant rooting depth

Land use type	z_0[m]	f_c [1] (min/max)	α_v [1] (jan/apr/jul/oct)	*LAI* [$m^2\ m^{-2}$] (min/max)	r_d [m]
Mixed forests^{pr,pa}	3.0	0.60/0.95	0.10/0.10/0.15/0.14	2.5/5.0	0.95
Open forests^{pr}	2.0	0.50/0.80	0.10/0.10/0.15/0.14	2.5/5.0	0.95
Shrubby forests^{pr}	1.0	0.50/0.80	0.10/0.10/0.15/0.14	1.0/2.0	0.95
Evergreen needleleaf forests^{pr}	8.0	0.80/0.90	0.09/0.10/0.10/0.10	6.0/8.0	0.95
Vineyards^{pr,pa}	0.2	0.30/0.70	0.16/0.18/0.20/0.16	0.5/1.8	0.60
Orchard^{pr}	0.5	0.30/0.70	0.16/0.18/0.20/0.16	1.0/2.0	0.60
Arable land^{pa}	0.05	0.20/0.80	0.19/0.25/0.25/0.22	0.5/3.0	0.50
Pasture (elevated zone)^{pr}	0.07	0.70/0.80	0.14/0.15/0.16/0.14	1.0/4.0	0.20
Meadow (long), croplands^{pr}	0.05	0.70/0.80	0.19/0.25/0.25/0.22	1.0/4.0	0.50
Meadow (short)^{pr}	0.01	0.70/0.80	0.20/0.26/0.26/0.23	1.0/4.0	0.30
Meadow (wet)^{pa}	0.07	0.70/0.80	0.12/0.12/0.16/0.15	0.5/3.0	0.50
Bog^{pr,pa}	0.15	0.40/0.80	0.13/0.13/0.18/0.16	1.0/2.0	0.70
Riparian zone, gravel^{pa}	0.5	0.25/0.50	0.12/0.15/0.15/0.12	0.5/1.5	0.80
Non vegetated^{pr}	0.01	−/−	−/−/−/−	−/−	−
Water^{pr,pa}	0.001	−/−	−/−/−/−	−/−	−
Closed shrublands^{pr}	0.7	0.50/0.70	0.12/0.15/0.15/0.12	1.0/2.0	0.80
Open shrublands^{pr}	0.5	0.40/0.50	0.12/0.15/0.15/0.12	1.0/1.5	0.80
Woody savannas^{pr}	1.0	0.60/0.80	0.12/0.15/0.15/0.12	1.0/2.0	0.80
City^{pr}	1.0	−/−	−/−/−/−	−/−	−
Village^{pr}	0.8	0.15/0.30	0.20/0.26/0.26/0.23	1.0/3.0	0.40
Building surroundings^{pr}	0.6	0.10/0.15	0.20/0.26/0.26/0.23	1.0/2.0	0.30
Parks^{pr}	0.05	0.30/0.50	0.20/0.26/0.26/0.23	1.0/2.0	0.40
Road, rail, airport^{pr}	0.015	0.10/0.15	0.20/0.26/0.26/0.23	1.0/2.0	0.40
Snow and ice^{pr}	10^{-5}	−/−	−/−/−/−	−/−	−

^{pr}present land use
^{pa}past land use

With the value of $c = 1.12$, f_v is 1 for 30% of the growing season. At the mean latitude of the study area ($\varphi = 47.0^\circ$), $D_v = 81.0$ days and $D_\tau = 223.5$ days.

The land-use and land-cover changes (present – past) in the study area resulted in a moderate decrease in the roughness length (−0.34 m in all months) and the plant rooting depth (−0.13m in all months). There were changes in the vegetation albedo (0.04, 0.08, 0.05, and 0.04 in JAJO, respectively) and there was an increase in the leaf area index (0.05, 0.18, 0.98, and 0.44 in JAJO, respectively) for all months. The change in the average vegetation albedo is highest in April at the beginning of the growing season, when the present-day agricultural vegetation is rather bright. In contrast, the past vegetation was dominated by plants which are more of an evergreen nature and therefore showed smaller changes in albedo throughout the year. The average increases in the total albedo, which takes into account the vegetation albedo and the bare soil albedo, were 0.03, 0.05, 0.04, and 0.03 in JAJO, respectively. The present-day fractional plant coverage is higher in January, April, and October (0.17, 0.14, and 0.09, respectively) and slightly lower in July (−0.02).

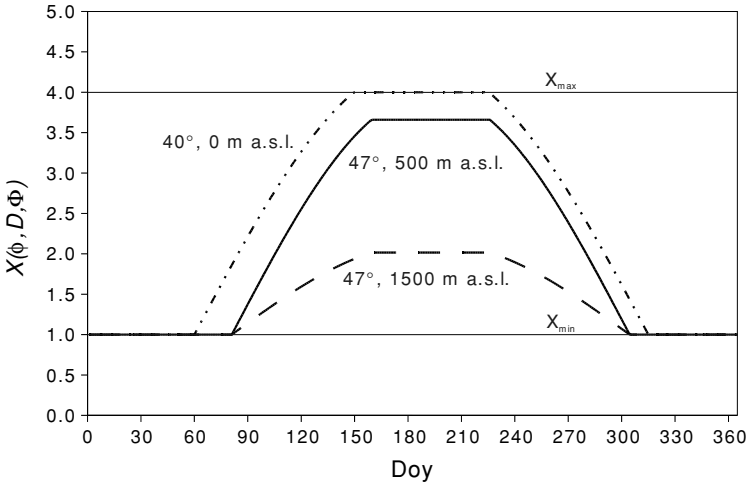

Fig. 11 Generic function X, which is used to parameterize the seasonal variation of the leaf area index and the fractional plant coverage, as a function of the day of year D, the latitude φ and the geopotential Φ. The solid line shows X for $\varphi = 47.0^\circ$ and an altitude of 500 m a.s.l., the dashed line shows X for the same latitude but 1500 m a.s.l. The dash-dotted line shows X for a location at sea level at $\varphi = 40.0^\circ$. Here, minimum and maximum values for X (e.g. leaf area index) are 1.0 and 4.0, respectively

Appendix B: Velocity scale

w_* is a velocity scale for the convective mixed layer. In order to calculate w_* according to Stull (1988), z_i must be known. z_i was calculated using the gradient Richardson number Ri as defined in Stull (1988). A critical Richardson number Ri_c of 0.38 was used to define the daytime mixed layer height where a transition from turbulent to laminar conditions with height occurs. The value of Ri_c was determined by the given choice of constants and length scales in the turbulence scheme and empirical validation (see Fay et al. 1997). w_* is typically on the order of 1 ms^{-1}, which is roughly the updraft speed in convective thermals.

References

Baidya Roy. S, Hurt GC, Weaver CP, Pacala SW (2003) Impact of historical land cover change on the July climate of the United States. J Geophys Res 108(D24):4793

Brown A (1999) Characterising prehistoric lowland environments using local pollen assemblages. J Quaternary Sci 14(6):585–594

CEC (1995) Wise use and conservation of wetlands. Communication from the Commission to the Council and the European Parliament. Commission of the European Communities (CEC), Brussels

Chase TN, Pielke RA, Kittel TGF, Nemani RR, Running SW (1996) The sensitivity of a general circulation model to global changes in leaf area index. J Geophys Res 101:7393–7408

Chase TN, Pielke RA, Kittel TGF, Nemani RR, Running SW (2000) Simulated impacts of historical land cover changes on global climate in northern winter. Clim Dynam 16:93–105

Chase TN, Pielke RA, Kittel TGF, Zhao M, Pitman AJ, Running SW, Nemani RR (2001) Relative climatic effects of landcover change and elvated carbon dioxide combined with aerosols: a comparison of model results and observations. J Geophys Res 106(D23):31,685–31,691

Clement R, Horn S (2001) Pre-Columbian land-use history in Costa Rica: a 3000-year record of forest clearance, agriculture and fires from Laguna Zoncho. Holocene 11(4):419–426

Cleugh HA, Raupach MR, Briggs PR, Coppin PA (2004) Regional-scale heat and water vapour fluxes in an agricultural landscape: an evaluation of CBL budget methods at oasis. Bound-Lay Meteorol 110:99–137

de Sherbinin A (2002) Land use and land cover change – a ciesin thematic guide. Center for International Earth Science Information Network, Columbia University, Palisades, NY

Eugster W, Siegrist F (2000) The influence of nocturnal CO_2 advection on CO_2 flux measurements. Basic Appl Ecol 1(2):177–188

Fay B, Schrodin R, Jacobsen I, Engelbart D (1997) Validation of mixing heights derived from the operational NWP models at the German Weather Service. In: S.-E. Gryning (ed): EURASAP workshop proceedings on The Determination of the Mixing Height – Current Progress and Problems pp 55–58

Frei E, Vökt U, Flückiger R, Brunner H, Schai F (1980) Bodeneignungskarte der Schweız 1:200'000. Bern: Eidg. Justiz- und Polizeidepartement, Bundesamt für Raumplanung

Fyfe R, Brown A, Rippon S (2003) Mid- to late-Holocene vegetation history of Greater Exmoor, UK: estimating the spatial extent of human-induced vegetation change. Veg Hist Archaeobot 12(4):215–232

Gobet E, Tinner W, Hochuli P, van Leeuwen J, Ammann B (2003) Middle to late holocene vegetation history of the upper Engadine (Swiss Alps): the role of man and fire. Veg Hist Archaeobot 12(3):143–163

Govindasamy B, Duffy PB, Caldeira K (2001) Land use changes and Northern Hemisphere cooling. Geophys Research Letters 28(2):291–294

Jahns S (2000) Late-glacial and Holocene woodland dynamics and land-use history of the lower Oder valley, north-eastern Germany, based on two, AMS C-14-dated, pollen profiles. Veg Hist Archaeobot 9(2):111–123

Kustas WP, Jackson TJ, Prueger JH, Hatfield JL, Anderson MC (2003) Remote sensing field experiments evaluate retrieval algorithms and land-atmosphere modeling. EOS 84(45):485–493

Loveland TR, Reed BC, Brown JF, Ohlen DO, Zhu J, Yang L, Merchant JW (2000) Development of a global land cover characteristics database and IGBP DISCover from 1-km AVHRR data. Int J Remote Sens 21(6/7):1303–1330

McNider RT, Kopp FJ (1990) Specification of the scale and magnitude of thermals used to initiate convection in cloud models. J Appl Meteorol 29:99–104

Mölders N (1999) On the effects of different flooding stages of the oder and different land-use types on the distributions of evapotranspiration, cloudiness and rainfall in the Brandenburg-Polish border area. Contr Atmos Phys 72(1):1–25

Mölders N (2000) Similarity of microclimate as simulated in response to landscapes of the 1930s and the 1980s. J Hydrometeorol 1:330–352

Ohlendorf C, Sturm M, Hausmann S (2003) Natural environmental changes and human impact reflected in sediments of a high alpine lake in Switzerland. J Paleolimnol 30(3):297–306

Pielke RA (2001) Influence of the spatial distribution of vegetation and soils on the prediction of cumulus convective rainfall. Rev Geophys 39:151–177

Pielke RA, Avissar R, Raupach M, Dolman JA, Zeng X, Denning AS (1998) Interactions between the atmosphere and terrestrial ecosystems: influcene on weather and climate. Global Change Biol 4:461–475

Pielke RA, Walko RL, Steyaert LT, Vidale PL, Liston GE, Lyons WA, Chase TN (1999) The influence of anthropogenic landscape changes on weather in South Florida. Mon Wea Rev 127:1663–1673

Poska A, Saarse L, Veski S (2004) Reflections of pre- and early-agrarian human impact in the pollen diagrams of Estonia. Palaeogeogr Palaeocl 209(1–4):37–50

Rabin, RM, Stadler S, Wetzel PJ, Stensrud DJ, Gregory M (1990) Observed effects of landscape variability on convective clouds. B Am Meteorol Soc 71:272–280

Schättler U, Doms G (1999) The interpolation program GME2LM: a user's guide. Offenbach: Deutscher Wetterdienst (DWD)

Schneider N, Eugster W (2005) Historical land use changes and mesoscale summer climate on the Swiss Plateau. J Geophys Res 110(D19102)

Schneider N, Eugster W, Schichler B (2004) The impact of historical land-use changes on the near-surface atmospheric conditions on the Swiss Plateau. Earth Interactions 8(12):1–27

Schrieber K, Stull R, Zhang Q (1996) Distributions of surface-layer buoyancy versus lifting condensation level over a heterogeneous land surface. J Atmos Sci 53(8):1086–1107

Segal M, Garratt JR, Kallos G, Pielke RA (1989) The impact of wet soil and canopy temperatures on daytime boundary-layer growth. J Atmos Sci 46(24):3673–3684

Smith EA, Hsu AY, Crosson WL, Field RT, Fritschen LJ, Gurney RJ, Kanemasu ET, Kustas WP, Nie D, Shuttleworth WJ, Stewart JB, Verma SB, Weaver HL, Wesely ML (1992) Area-averaged surface fluxes and their time-space variability over the FIFE experimental domain. J Geophys Res 97(D17):18599–18622

Stewart JB, Verma SB (1992) Comparison of surface fluxes and conductances at two contrasting sites within the FIFE area. J Geophys Res 97(D17):18623–18628

Stohlgren TJ, Chase TN, Pielke RA, Kittel TGF, Baron JS (1998) Evidence that local land use practices influence regional climate, vegetation, and stream flow patterns in adjacent natural areas. Global Change Biol 4:495–504

Stull RB (1988) Boundary layer meteorology. Dordrecht: Kluwer Academic Publishers

Venäläinen A, Rontu L, Solantie R (1999) On the influence of peatland draining on local climate. Boreal Environ Res 4:89–100